Data-Driven Phosphine Ligand Design of Ni-Catalyzed Enantioselective Suzuki–Miyaura Cross-Coupling Reaction for the Synthesis of Biaryl Atropisomers: standing on the shoulder of Pd catalysis giants

Xin-Yuan Xu[a‡], Li-Cheng Xu[a‡], Li-Gao Liu[a‡], Ping Lu [a], Shuo-Qing Zhang[a*], and Xin Hong[abc*]

[a] Center of Chemistry for Frontier Technologies, Department of Chemistry, State Key Laboratory of Clean Energy Utilization, Zhejiang University, Hangzhou 310027, China.
[b] Beijing National Laboratory for Molecular Sciences, Zhongguancun North First Street NO. 2, Beijing 100190, P.R. China
[c] State Key Laboratory of Physical Chemistry of Solid Surfaces, Xiamen University, Xiamen 361005, P.R. China
[‡] These authors contributed equally.

Abstract: The Suzuki-Miyaura cross-coupling reaction is a cornerstone in organic synthesis, enabling the formation of carbon–carbon bonds with high efficiency and selectivity. This study represents a groundbreaking advancement in the field by pioneering the first enantioselective Ni-catalyzed Suzuki–Miyaura cross-coupling reactions for the synthesis of biaryl atropisomers. Employing a data-driven approach, we have crafted a novel *N*-protected Xiao-Phos ligand, which, in conjunction with commercially available $Ni(COD)_2$, delivered unparalleled enantioselectivity and reactivity under mild conditions. The ligand design was meticulously guided by an extensive examination of the existing literature on Pd-catalyzed asymmetric Suzuki–Miyaura cross-coupling reactions, directing the virtual screening and subsequent experimental verification of the synthesized ligands in a single iteration. The innovative ligand *N*-Bn-Xiao-Phos exhibited impressive enantioselectivities coupled with exceptional yields, showcasing versatility with a diverse array of functional groups and aryl boronic acids, and accomplishing successful gram-scale synthesis. DFT computational studies provided profound insights into the reaction mechanism and the roots of enantioselectivity, elucidating the dynamic coordination modes of the chiral ligand and the steric induction. This breakthrough not only broadens the horizons of Ni-catalyzed cross-coupling reactions but also highlights the immense potential of machine learning in the judicious design of chiral ligands for asymmetric synthesis.

INTRODUCTION

In the past few decades, the Suzuki–Miyaura cross-coupling (SMC) reaction has emerged as the most commonly employed method among the array of cross-coupling reactions[1]. More recently, the development of sophisticated novel ligands has led to the advent of enantioselective variants of the Pd-catalyzed Suzuki–Miyaura Cross-coupling reaction, enabling the synthesis of a diverse array of biaryl atropisomers (Fig.1A)[2]. In 2000, the pioneering reports of the groups Cammidge[3] and Buckwald[4] on Pd-catalyzed asymmetric SMC reactions demonstrated the possibility of utilizing substrates and/or chiral ligands enabled enantio-convergent transformation to gain access to biaryl atropisomers from commercially available and bench-stable substrates. Since then, tremendous progress has been made in this

field and a series of phosphine, bis-Hydrazone, N-heterocyclic carbene (NHC) and diene based chiral ligands were developed by groups of Qiu[5], Wu and Zhang[6], Tang[7], Byrne and Smith[8], Fernández and Lassaletta[9], Lin[10], Dorta[11] and Shi[12] to improve enantioselectivity as well as expand the substrate scope of asymmetric Pd-SMC. In addition, various novel approaches introducing bio[13] or heterogeneous[14] catalysis have been proved to achieve moderate to excellent enantiocontrol.

Concomitantly, Ni-catalyzed cross-coupling reactions have been gathering momentum, offering a more abundant and cost-effective alternative[15]. These have rendered significant contributions to a variety of synthetic pathways[16]. However, the burgeoning field of Ni-catalyzed reactions is currently tilting towards radical-mediated processes[17], thereby leaving the synergy between Ni and Pd, as well as the exploitation of chiral phosphine ligands in Ni catalysis, largely unexplored.

Over the past two decades, since the introduction of Pd-SMC, extensive research has been undertaken to explore the application of Ni-SMC for the synthesis of biaryl derivatives[18], along with computational studies that have aimed to elucidate the mechanism of this transformation, including contributions from our group (Fig.1B)[18g,19]. Most recently, Diao et al. have designed a novel ProPhos ligand for racemic Ni-catalyzed Suzuki–Miyaura cross-coupling reactions, emphasizing the acceleration of the pivotal transmetalation step[20].

Despite these recent advancements, the enantioselective synthesis of biaryl atropisomers using Ni-SMC remains an unexplored area for organic chemists, to the best of our knowledge. This approach is currently hampered by the lower reactivity of Ni catalysts relative to Pd, which necessitates higher catalyst loadings (typically over 5%)[21] and higher reaction temperatures (generally above 60 °C)[18d], which can significantly complicate enantioselective control. Moreover, the reported reactivity scope for Ni-SMC is limited, with di-ortho-substituted biaryl products being scarcely documented, and the requirement for at least tri-ortho-substituted substrates to generate stable atropisomers. Nevertheless, we postulate that these challenges can be addressed through the meticulous design of chiral ligands and a comprehensive investigation of the reaction conditions.

In recent years, the advent of data-driven approaches has begun to reshape the landscape of reaction methodology development and optimization[22]. The transfer of knowledge from previously established reactions has shown immense potential in advancing the frontiers of new reaction methodologies[22d,23].

Herein, we present the first enantioselective Ni-catalyzed Suzuki–Miyaura cross-coupling reactions for the synthesis of biaryl atropisomers based on a transferring machine learning from reported Pd-catalyzed Suzuki–Miyaura cross-coupling reactions, where we modified the commercially available Xiao-Phos relying on a data-driven workflow (Fig.1C). With this workflow, we obtained excellent yields and enantioselectivity with the novelly designed *N*-protected Xiao-Phos ligand under mild reaction conditions, and the origins of enantioselectivity was elucidated to be steric effects by DFT calculations.

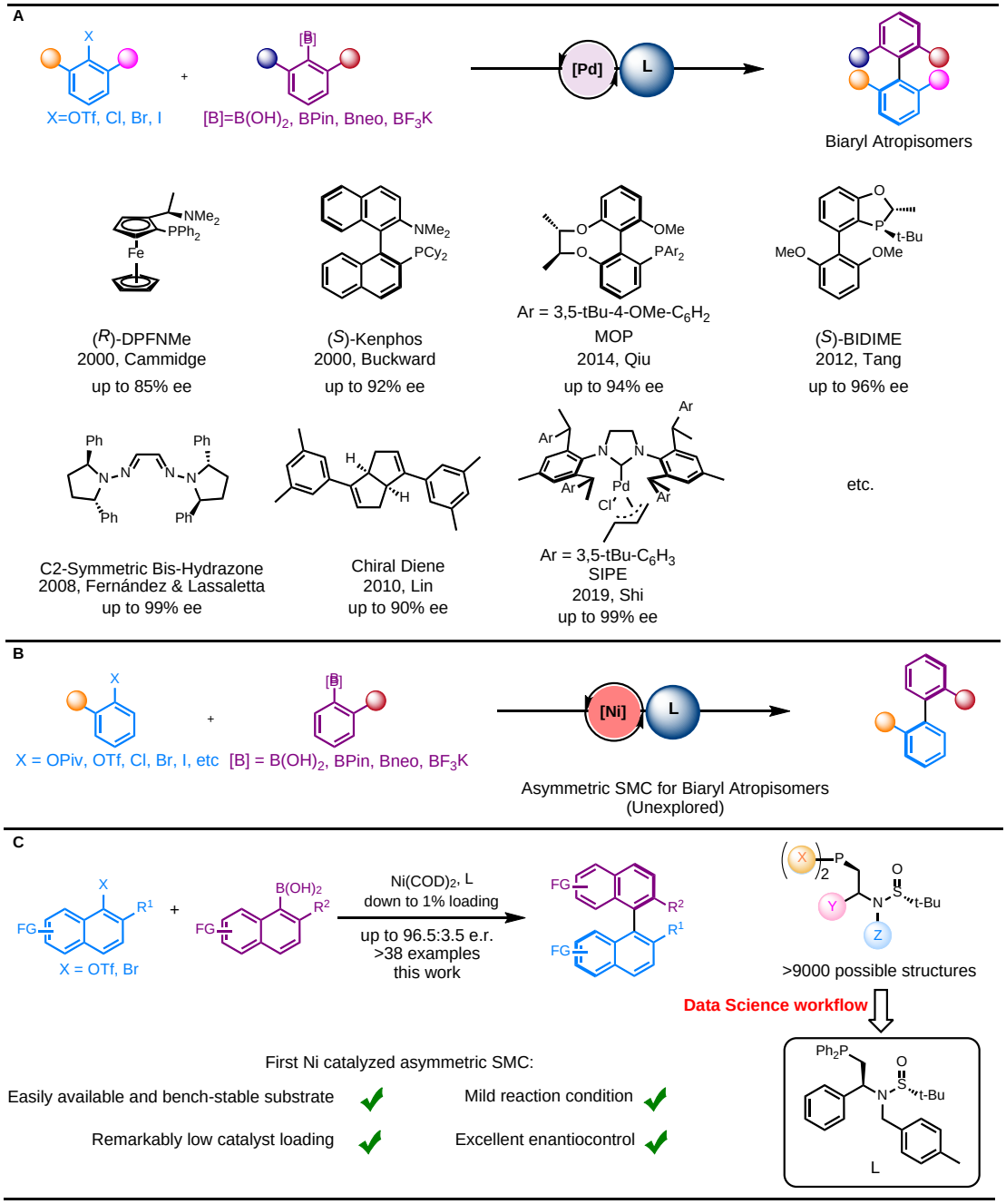

Fig. 1 | Background for asymmetric SMC and our strategy: A. Asymmetric Pd-SMC for biaryl atropisomers synthesis and representative ligands involved. **B**. Current state of Ni-SMC. **C**. The first enantioselective Ni-SMC for the synthesis of biaryl atropisomers based on data-driven workflow for ligand design.

RESULTS AND DISCUSSION

Reaction condition optimization and preliminary ligand scaffold screening

To commence our study, a meticulous optimization of the racemic reaction conditions using PCy_3 or PPh_3 as ligands was conducted (see Table S2 in the Supporting Information for more details). Based on the precedent for Ni-catalyzed Suzuki–Miyaura cross-coupling reaction methodologies[18], our study delightedly uncovered that N, N-dimethylformamide (DMF) is an optimal solvent when paired with triphenylphosphine (PPh_3) ligand. The use of potassium

phosphate (K_3PO_4) as the base, $Ni(COD)_2$ as the catalyst precursor, under a nitrogen atmosphere, and a temperature regime of 80 °C for a duration of 12 hours yielded an impressive 89% conversion rate.

Having established the reaction conditions, we embarked on a screening using a subset of 19 commonly encountered and readily available chiral phosphine ligands (see Table S3 in the Supporting Information for more details). Unfortunately, none of the tested reactions exhibited high enantioselectivity. Nevertheless, among the ligands investigated, those based on the family of Sadphos scaffold[24] exhibited considerable promise, demonstrating some reactivity and enantioselectivity. Furthermore, their modular synthetic strategy provides flexibility and ease of manipulation, laying the groundwork for further ligand optimization and exploration in further data-driven ligand design. Consequently, we evaluated numerous other commercially available Sadphos ligands, only to be disappointed by the continued lack of satisfactory outcomes. (see Table S4 in the Supporting Information for more details) This outcome motivated us to pursue a more sophisticated ligand design strategy.

Data-driven Ligand Design and Evaluation

To initiate our investigation into ligand design, we further compiled 21 data points for Ni-catalyzed asymmetric Suzuki–Miyaura cross-coupling reactions utilizing less commercially available yet purchasable Sadphos ligands (see Table S6 in the Supporting Information for more details). Acknowledging the intricacies of enantioselectivity, we anticipated that a more extensive dataset would be beneficial and pivotal for a successful ligand design. Considering that both Ni and Pd catalysis share similar mechanisms in Suzuki–Miyaura cross-coupling reactions, we envisioned that the knowledge from the well-established Pd-catalyzed asymmetric Suzuki–Miyaura cross-coupling reactions could serve as a valuable data source. Consequently, we initially curated a dataset from 23 literature sources on Pd-catalyzed asymmetric Suzuki–Miyaura cross-coupling reactions published after the year 2000. This dataset encompasses a total of 311 reaction records, including 29 halides, 15 boronic acids, and 101 ligands. The enantiomeric excess (ee) values and Gibbs free energy differences were appropriately distributed. (Figure 1) Notably, the highest achieved ee value was 99%.

Building upon the data obtained from the collected dataset of Pd catalysis and 21 data for Ni catalysis with Sadphos ligands, we have developed a comprehensive workflow for the virtual screening of ligands tailored for the model Ni-catalyzed asymmetric Suzuki–Miyaura cross-coupling reaction, where the substrates **1** and **2,** as well as the reaction conditions were maintained constant, allowing for a more focused investigation on the ligand's influence on the enantioselectivity. The workflow is structured around four principal stages (Figure 2).

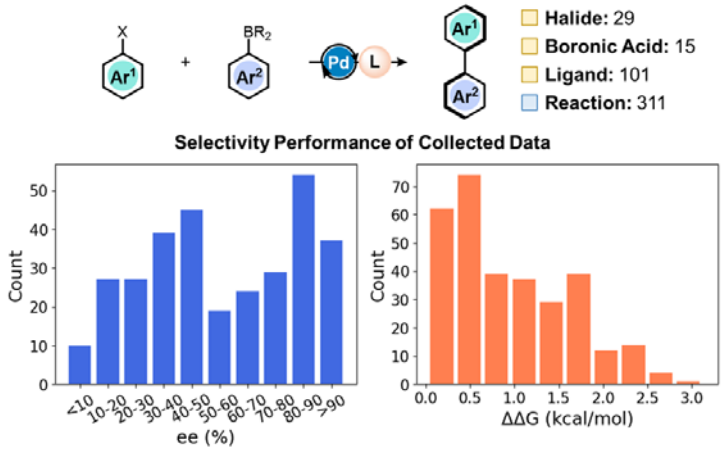

Fig. 2 | Statistics of collected data on Pd-catalyzed Suzuki–Miyaura cross-coupling reactions.

1. **Generation of Virtual Ligand Library:** The generation of virtual ligand library was developed based on the specific Sadphos scaffold, incorporating R^1 substituents, R^2 substituents, and R^3 substituents. This library comprises a vast collection of structures, amounting to a size of several thousand entities (see Fig. S1 in the Supporting Information for more details).
2. **Generation of Reaction Encodings:** The generation of reaction encodings involves the creation of digital representations for the reactions extracted from the literature, the data obtained from the Sadphos ligand screening process, and the corresponding data for each ligand within the virtual ligand library. Specifically, we commenced by constructing molecular graphs of the key reaction intermediates featuring aryl groups from the halogenated aryl substrates, aryl groups from boronic acid substrates, and bidentate chiral ligands associated with the square planar Pd or Ni center. Subsequently, we computed the Morgan molecular fingerprints of these intermediate molecules to facilitate the digital encoding of the reactions. This encoding scheme allows for the thorough characterization and comparison of the selectivity of various ligands in asymmetric Suzuki–Miyaura cross-coupling reactions.
3. **Training of Virtual Ligand Predictor:** The training of the virtual ligand library screening model involves a refined version of our previously developed hierarchical learning strategy.[25] For each reaction in the virtual ligand library, we employed Morgan fingerprint similarity to extract reaction data from the pool of Pd literature dataset that share enough similarity with the virtual reaction. These data were used to train a base model capable of capturing the simple structure-activity relationships of the reactions. Subsequently, a delta model is trained using a small amount of the Ni-catalyzed reaction data generated during Sadphos ligand screening process, aiming to fit the residuals between the base model's predicted values and the actual values. The enantioselectivity prediction for the virtual reaction is then obtained by summing the predictions from both the base and delta models. In this manner, each virtual ligand is associated with a distinct predictor that is tailored to its specific characteristics, consisting of a customized base model and an accompanying delta model.

   The optimization of the virtual ligand library prediction model involves the selection of optimal hyperparameters to ensure the most accurate predictions. To this end, we have chosen a subset of several machine learning algorithms, several similarity assessment

methods, and several similarity thresholds (see Table S1 in the Supporting Information for more details). Utilizing a dataset of 311 Pd catalysis literature reactions alongside 21 Ni-catalyzed reaction data generated during Sadphos ligand screening process, we identified the optimal model hyperparameters. The selection criterion for these hyperparameters was based on the leave-one-out (LOO) Pearson R correlation coefficient for the 21 target reactions in relation to the reaction conditions screening.

4. **Ligand Ranking and Experimental Evaluation:** The virtual ligand experimental evaluation was initiated by computing the synthesizability of all virtual ligands. Ligands with a SAScore[26] greater than 4.0 were set as less prior ligands due to their less synthesize accessibility in the first round for more robust availability in the experimental ligand syntheses. An evaluation metric that incorporates both the model's predictions of enantioselectivity and the synthesizability of the ligands (SAScore) is used to determine which ligands should be synthesized and eventually experimentally validated. The ligand predictor will be retrained with the fresh additional experimental evaluation data and the loop will be repeated unless the outcome of the experimental evaluation is satisfactory.

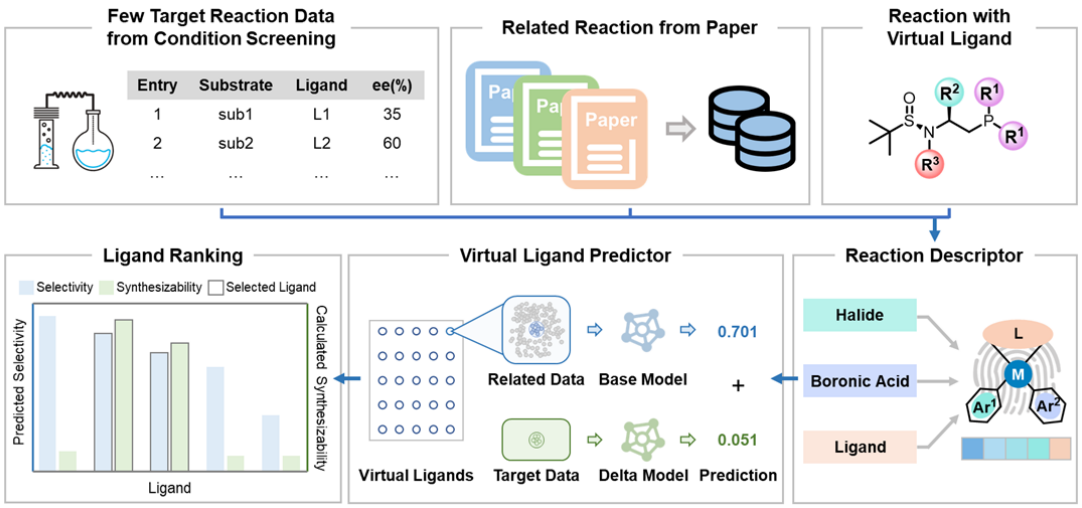

Fig. 3 | Workflow of data-driven virtual ligand design for Ni-catalyzed Suzuki–Miyaura reactions.

Upon conducting the first iteration of virtual ligand screening, we were pleased to uncover a promising result: the readily accessible N-aryl-protected Xiao-Phos ligands exhibited an impressive degree of enantioselectivity. As shown in Table 1A, the syntheses of **L1**, **L2**, and **L3** was achieved with 3 steps, yielding satisfactory productivities. The absolute configuration of **L3** was unambiguously determined by X-ray crystallographic analysis, and its chirality was preserved throughout the synthesis. Equipped with these novel ligands, we were able to assess their catalytic performances (Table 1B). Consistent with the virtual ligand screening predictions, both **L1** and **L3** exhibited noteworthy enantioselectivities of 91% and 93%, respectively. Moreover, **L3** also showcased exceptional reactivity, culminating in an outstanding yield of 95%. These outcomes validate the efficacy of our ligand design approach, requiring only a single iteration to achieve success.

Exploration of substrate scopes and synthetic applications

In possession of a potent catalytic system (**L3**), we ventured into the realm of enantioselective synthesis of biaryl atropisomers. Given the remarkable reactivity of **L3**, we explored the impact of reducing the reaction temperature from 80 °C to room temperature in search of enhanced enantioselectivity. Pleasingly, the reaction progressed smoothly at the reduced temperature, prompting us to establish room temperature as the optimal condition for the reaction.

Our initial focus was on the substrate scope of aryl boronic acids (Table 2). We were pleased to discover that both electron-withdrawing and electron-donating substituents were accommodated without compromising enantioselectivity (compounds **4** to **8**). The absolute configuration of **5** was confirmed to be XX by X-ray crystallographic analysis. Furthermore, we found that extended conjugated aromatic ring systems could be tolerated, again with no loss of enantioselectivity (compounds **9** to **13**). Additionally, S-containing heterocycles were also compatible with our catalytic system, maintaining high levels of enantioselectivity (compounds **14** and **15**).

Table 1 | Synthesis and validation of predicted top-3 ligands

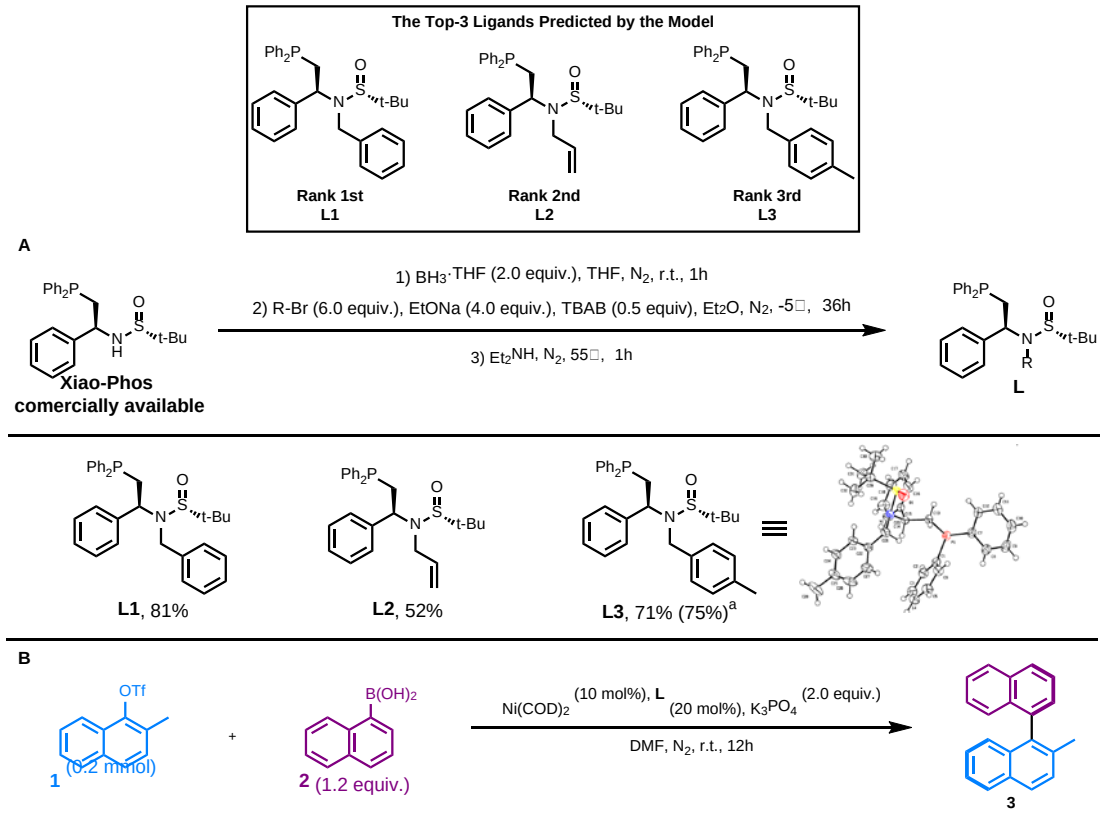

Entry	L	Yield (%)	e.r. (%)
1	**L1**	85	95.5:4.5
2	**L2**	35	88.5:11.5
3	**L3**	95	96.5:3.5
4[b]	**L3**	91 (89)[c]	96:4

A. Synthesis of the ligands. Reactions were performed on a 0.2 mmol scale. The absolute configuration of **L1** was confirmed by X-ray crystallographic analysis. **B.** Validation of the synthesized ligands. Reactions were performed on a 0.2 mmol scale. Yield is based on ^{1}H-NMR analysis of the crude product using CH_2Br_2 as an internal standard. E.r. of **3** is based on HPLC analysis. [a]Yields on 2.0 mmol scale. [b]Reactions were performed on 0.4 mmol scale. $Ni(COD)_2$ (1 mol%), **L1** (2 mol%), solvent = Toluene/DMF(v/v = 10/1). [c]Isolated yields.

Table 2 | Substrate scopes of aryl boronic acids

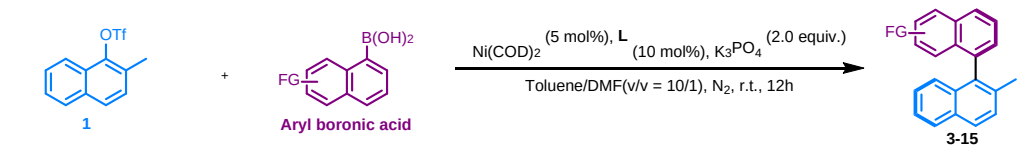

Scope of Aryl boronic acid

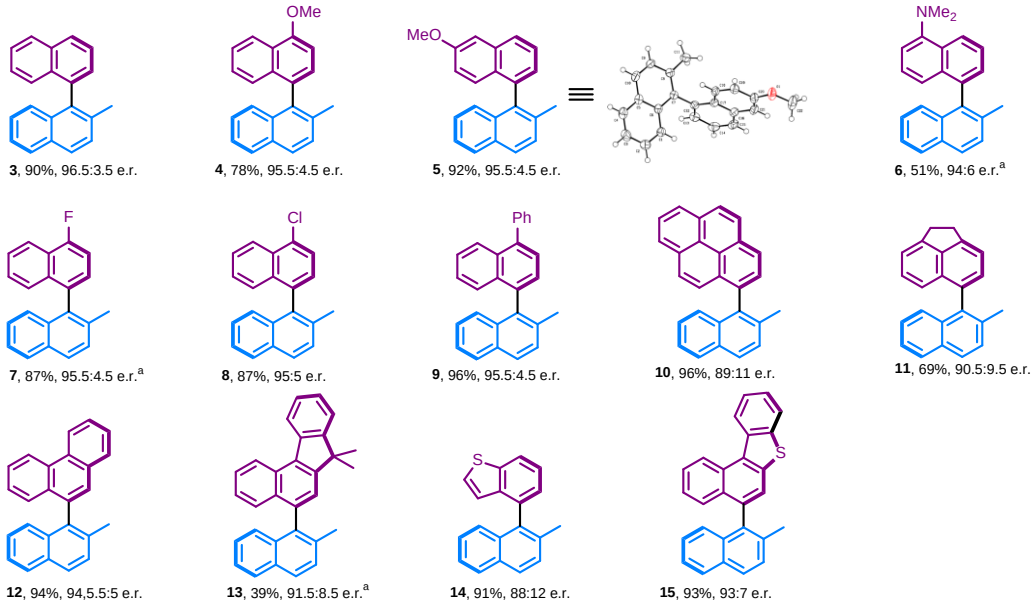

3, 90%, 96.5:3.5 e.r.
4, 78%, 95.5:4.5 e.r.
5, 92%, 95.5:4.5 e.r.
6, 51%, 94:6 e.r.[a]
7, 87%, 95.5:4.5 e.r.[a]
8, 87%, 95:5 e.r.
9, 96%, 95.5:4.5 e.r.
10, 96%, 89:11 e.r.
11, 69%, 90.5:9.5 e.r.
12, 94%, 94,5.5:5 e.r.
13, 39%, 91.5:8.5 e.r.[a]
14, 91%, 88:12 e.r.
15, 93%, 93:7 e.r.

Reactions were performed on 0.2 mmol scale. E.r.s of **3**-**15** were based on HPLC analysis. The absolute configuration of **5** was confirmed by X-ray crystallographic analysis. [a]$Ni(COD)_2$ (10 mol%), **L3** (20 mol%)

Our subsequent investigation centered on the substrate scope of aryl triflates and aryl bromides (Table 3). We observed that aryl groups bearing moderate steric demand at the ortho-positions were well-tolerated by the catalyst (compounds **16** to **18**). Additionally, the introduction of both electron-withdrawing and electron-donating substituents at various positions on the aryl ring did not adversely affect the enantioselectivity of the reaction (compounds **19** to **35**). A variety of functional groups, including ethers, esters, aldehydes, ketones, sulfonamides, and amines, were found to be compatible with the reaction conditions, again with no loss of enantioselectivity (compounds **20** to **30**). Furthermore, reactive substituents such as –F or –Cl were also accommodated (compounds **31** to **33**), and allyl substitutions remained intact throughout the reaction process (compound **35**). Importantly, the catalytic system demonstrated compatibility with extended conjugated aromatic ring systems, preserving high levels of enantioselectivity (compounds **36** and **40**).

Table 3 | Substrate scopes of aryl triflate or aryl bromide

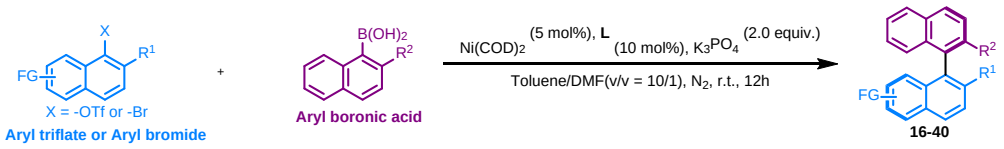

Scope of Aryl triflate or Aryl bromide (R^2 = H or Me)

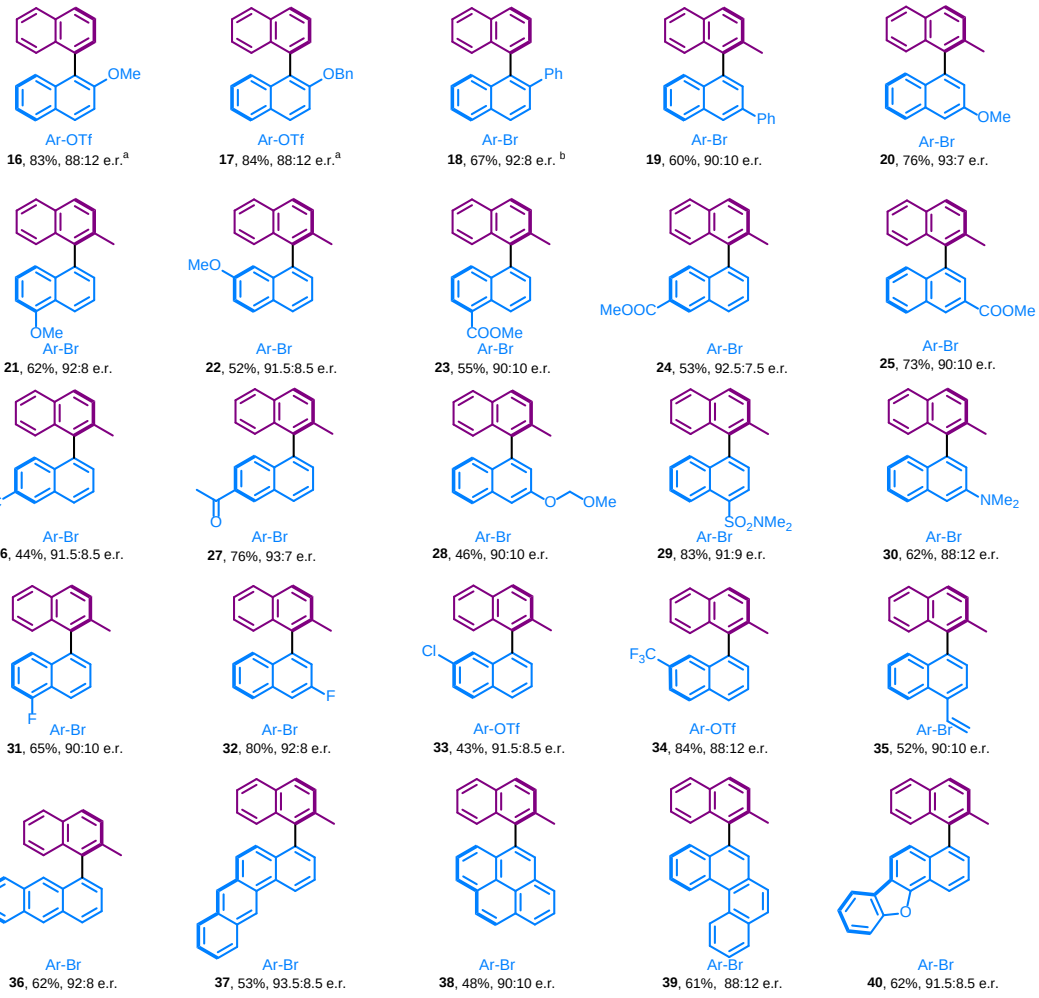

Reactions were performed on 0.2 mmol scale. E.r.s of **16-40** were based on HPLC analysis. [a]Reactions were performed on 0.4 mmol scale at room temperature. $Ni(COD)_2$ (1 mol%), **L3** (2 mol%). [b]Reactions were performed at room temperature. $Ni(COD)_2$ (5 mol%), **L1** (10 mol%).

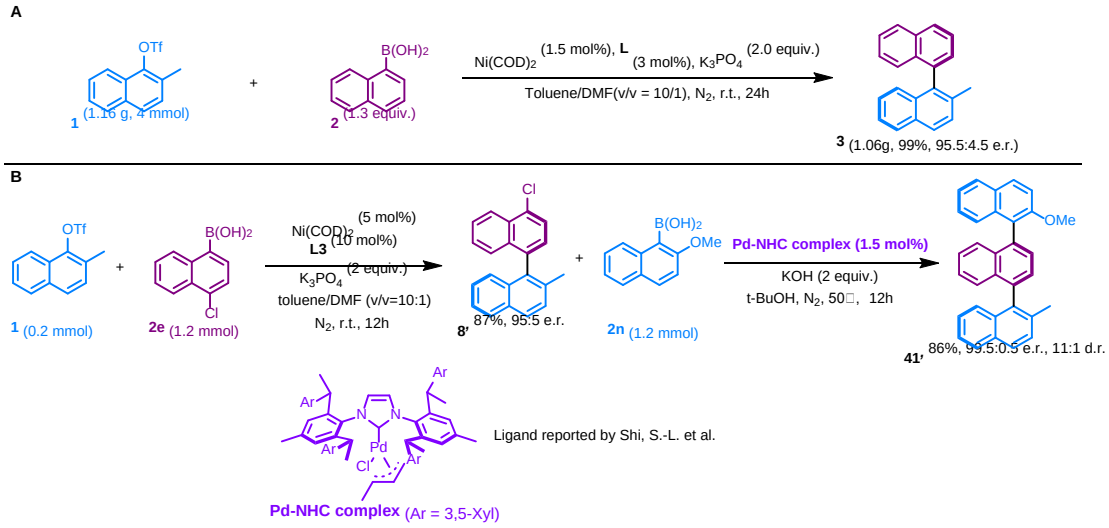

Fig. 4 | Synthetic application. A, Gram-scale synthesis. E.r. of **3** was based on HPLC analysis. **B,** Synthesis of axially chiral ternaphthalenes. E.r. of **3** was based on HPLC analysis. D.r. of **3** was determined by ^{1}H NMR and confirmed by HPLC analysis.

In the pursuit of synthetic applications, the axially chiral binaphthalene **3** was successfully scaled up to the gram-scale under optimal reaction conditions, yielding in 99% yield with an e.r. of 95.5:4.5 (Figure 4A). Notably, the catalyst loading for this gram-scale synthesis was remarkably low at just 1.5 mol%, which underscores the superior catalytic efficiency of the newly designed ligand **L3**. Capitalizing on the distinctive stability of the –Cl substituent in our methodology, we successfully synthesized axially chiral ternaphthalenes through a sequential Ni and Pd catalysis process (Figure 4B). **1** reacted with **2e** to yield **8** under standard reaction conditions, with an e.r. of 95:5. Subsequently, **8** underwent reaction with **2n** to produce the chiral ternaphthalene **41** under the standard conditions reported by Shi et al.[12], achieving an outstanding e.r. of 99.5:0.5 and a favorable d.r. of 11:1. This sequential synthesis showcases the potential for the synthesis of complex axially chiral conjugated aryl ring systems by Suzuki–Miyaura cross-coupling reactions.

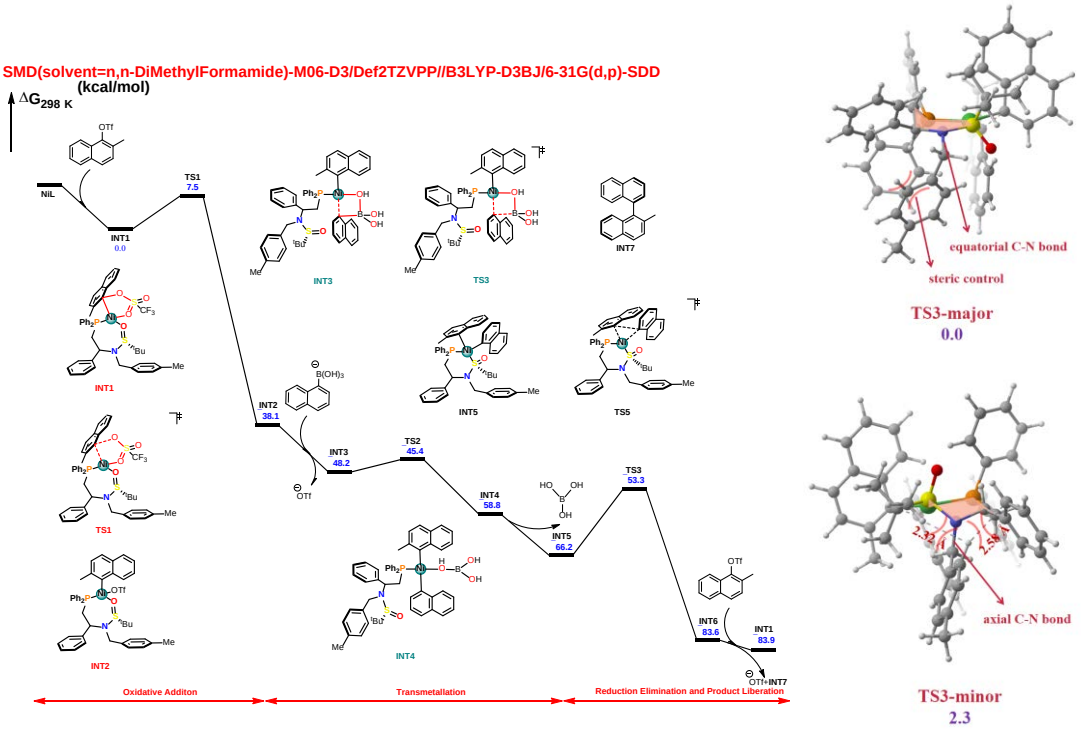

Fig. 5 | DFT-computed free energy diagram for Ni-catalyzed Suzuki–Miyaura cross-coupling reactions.

Computational Study

Building upon the ligand design and experimental outcomes, we carried out detailed DFT computations to elucidate the mechanism of the Suzuki–Miyaura cross-coupling reaction and the origin of its remarkable enantioselectivity. The DFT-computed free energy profile of Ni/**L1**-catalyzed Suzuki-Miyaura cross-coupling between **1** and **2** is shown in Figure 5. From the substrate-coordinated complex **INT1**, the oxidative addition of 2-methylnaphthalen-1-yl triflate **2** through **TS1** is very facile with a free energy barrier of 7.5 kcal/mol, thereby forming the aryl–nickel intermediate **INT2**. In these processes, **L1** functions as a bidentate ligand with P and O atoms serving as the coordinating atoms. Afterward, **INT2** readily dissociates the tethered sulfinyl group to engage the hydroxy(naphthalen)borate **2-OH**, giving rise to **INT3** with loss of OTf^- anion, and thus facilitating the subsequent transmetallation process via an outer-sphere mechanism through **TS2**, which requires a free energy barrier of only 2.8 kcal/mol. The acceleration of transmetalation was also acknowledged and proved pivotal very recently in Ni-catalyzed Suzuki–Miyaura cross-coupling reactions.[Diao] The directly formed **INT4** undergoes the dissociation of $B(OH)_3$ and re-coordination of S atom in the sulfinyl group, affording the more stable bi-aryl – nickel intermediate **INT5**. Finally, compound **INT5** undergoes an aryl-aryl reductive elimination step through **TS3** leading to the product-coordinated complex **INT6**. Subsequent product (**3**) liberation and coordination of substrate **1** regenerates the active nickel intermediate **INT1** and thus completes the catalytic cycle. The computed catalytic cycle is in good accordance with the fact that the reaction proceeds smoothly under mild conditions, and the aryl-aryl reductive elimination step is the rate-determining step. Furthermore, our DFT computations reveal that the coordination modes of the chiral ligand **L1** with the metal center are dynamic and evolve throughout the reaction

stages, potentially accelerating the catalytic process. (see Fig. S2 in the Supporting Information for more details). These findings suggest that the chameleon-like coordinating ability of **L1** may be envisioned for broader and more versatile applications in analogous catalytic reactions.

The free energy profiles presented herein allow us to deduce that the irreversible aryl-aryl reductive elimination step, occurring through the transition state **TS3**, is the pivotal enantio-determining step. The computed free energy difference of 2.3 kcal/mol between the **TS3-major** and **TS3-minor** transition states correlates well with the experimentally observed *e.r.* value of 93%. A detailed analysis of the structures at the two enantioselective transition states reveals that the differential configuration and orientation of the benzyl group within these transition states are responsible for the enantioselectivity. Specifically, within the highlight six-membered ring, steric repulsions between the benzyl group and the surrounding branched groups in **TS3-minor** lead to a less stable axial C–N bond compared to the more energetically favored equatorial C–N bond observed in **TS3-major**. This steric interference plays a crucial role in dictating the enantioselectivity of the reaction and highlights the importance of the N-protecting group identified in the ligand design stage.

CONCLUSIONS

We have successfully achieved a seminal advance in the realm of asymmetric synthesis by developing the first enantioselective Ni-catalyzed Suzuki–Miyaura cross-coupling reactions for the preparation of biaryl atropisomers. The meticulously optimized reaction conditions, coupled with the innovative *N*-protected Xiao-Phos ligand, have yielded a highly efficient and enantioselective catalytic system. The exploration of the substrate scope has revealed the tolerance of the catalytic system to a variety of functional groups and aryl boronic acids, further emphasizing the practicality of this method for complex molecule synthesis. The gram-scale synthesis of axially chiral binaphthalenes showcases the scalability of the process and the potential for industrial applications. Computational studies have shed light on the reaction mechanism, providing insights into the dynamic coordination modes of the chiral ligand and the pivotal role of the N-protecting group in enantioselectivity.

Our virtual screening approach, informed by a comprehensive analysis of Pd-catalyzed reactions, has not only expedited the ligand design process but has also provided a blueprint for future ligand development in asymmetric catalysis. The data-driven ligand design strategy employed has proven to be a powerful tool for the rational development of chiral ligands, significantly reducing the trial-and-error associated with traditional ligand discovery. Looking ahead, this work sets the stage for several exciting avenues of research. The ability to predict reaction outcomes and optimize conditions with minimal experimental work will greatly accelerate the discovery of new synthetic routes and the development of novel catalysts. Additionally, the exploration of this catalytic system in other asymmetric transformations, such as asymmetric hydrogenation or allylic substitution, could lead to new synthetic methodologies with broad applicability. Furthermore, the extension of this approach to other cross-coupling reactions could provide a versatile platform for the synthesis of a wide array of chiral compounds. The combination of experimental innovation, computational analysis, and data-driven design principles has the potential to transform the way we approach the synthesis of complex chiral molecules, offering a more efficient, predictable, and sustainable

approach to the creation of pharmaceuticals, agrochemicals, and materials.

ACKNOWLEMENT

National Key R&D Program of China (2022YFA1504301, X. H.), National Natural Science Foundation of China (22122109 and 22271253, X. H.; 22103070, S.-Q. Z.), Zhejiang Provincial Natural Science Foundation of China under Grant No. LDQ23B020002 (X. H.), the Starry Night Science Fund of Zhejiang University Shanghai Institute for Advanced Study (SN-ZJU-SIAS-006, X. H.), Beijing National Laboratory for Molecular Sciences (BNLMS202102, X. H.), CAS Youth Interdisciplinary Team (JCTD-2021-11, X. H.), Fundamental Research Funds for the Central Universities (226-2022-00140, 226-2022-00224 and 226-2023-00115, X. H), the State Key Laboratory of Clean Energy Utilization (ZJUCEU2020007, X. H.), the State Key Laboratory of Physical Chemistry of Solid Surfaces (202210, X. H.), the Leading Innovation Team grant from Department of Science and Technology of Zhejiang Province (2022R01005, X. H.) are gratefully acknowledged. Calculations were performed on the high-performance computing system at Department of Chemistry, Zhejiang University.

REFERENCES

1. For selected review on SMC: (a) Miyaura, N.; Suzuki, A. Palladium-Catalyzed Cross-Coupling Reactions of Organoboron Compounds. *Chem. Rev.* **95**, 2457(1995). (b) Baudoin, O. The Asymmetric Suzuki Coupling Route to Axially Chiral Biaryls. *Eur. J. Org. Chem.* **2005**, 4223–4229(2005). (c) Zhang, D.; Wang, Q. Palladium Catalyzed Asymmetric Suzuki–Miyaura Coupling Reactions to Axially Chiral Biaryl Compounds: Chiral Ligands and Recent Advances. *Coord. Chem. Rev.* **286**, 1–16(2015). (d) Li, C.; Chen, D.; Tang, W. Addressing the Challenges in Suzuki–Miyaura Cross-Couplings by Ligand Design. *Synlett* **27**, 2183–2200(2016).
2. Gaspard Hedouin, G.; Hazra, S.; Gallou, F.; Handa, S. The Catalytic Formation of Atropisomers and Stereocenters via Asymmetric Suzuki–Miyaura Couplings. *ACS Catal.* **12**, 4918–4937(2022)
3. Cammidge, A. N.; Crépy, K. V. L. The First Asymmetric Suzuki Cross-Coupling Reaction. *Chem. Commun.* **18**, 1723–1724(2000).
4. Yin, J.-J.; Buchwald, S. L. A Catalytic Asymmetric Suzuki Coupling for the Synthesis of Axially Chiral Biaryl Compounds. *J. Am. Chem. Soc.* **122**, 12051–12052(2000).
5. (a) Wang, S.-L.; Li, J.-J.; Miao, T.-T.; Wu, W.-H.; Li, Q.; Zhuang, Y.; Zhou, Z.-Y.; Qiu, L.-Q. Highly Efficient Synthesis of a Class of Novel Chiral-Bridged Atropisomeric Monophosphine Ligands via Simple Desymmetrization and Their Applications in Asymmetric Suzuki–Miyaura Coupling Reaction. *Org. Lett.* **14**, 1966–1969(2012). (b) Wu, W.-H.; Wang, S.-L.; Zhou, Y.-G.; He, Y.-W.; Zhuang, Y.; Li, L.-N.; Wan, P.; Wang, L.-S.; Zhou, Z.-Y.; Qiu, L.-Q. Highly Diastereoselective Synthesis of Atropisomeric Bridged P,N-Ligands and Their Applications in Asymmetric Suzuki–Miyaura Coupling Reaction. *Adv. Synth. Catal.* **354**, 2395–2402(2012). (c) Zhou, Y.-G.; Wang, S.-L.; Wu, W.-H.; Li, Q.; He, Y.-W.; Zhuang, Y.; Li, L.-N.; Pang, J.-Y.; Zhou, Z.-Y.; Qiu, L.-Q. Enantioselective Synthesis of Axially Chiral Multifunctionalized Biaryls via Asymmetric Suzuki–Miyaura Coupling. *Org. Lett.* **15**, 5508–5511(2013). (d) Zhou, Y.-G.; Zhang, X.-P.; Liang, H.-Y.; Cao, Z.-K.; Zhao, X.-Y.; He, Y.-W.; Wang, S.-L.; Pang, J.-Y.; Zhou, Z.-Y.; Ke, Z.-F.; Qiu, L.-Q. Enantioselective Synthesis of

Axially Chiral Biaryl Monophosphine Oxides via Direct Asymmetric Suzuki Coupling and DFT Investigations of the Enantioselectivity. *ACS Catal.* **4**, 1390−1397(2014). (e) Li, Y.-S.; Pan, B.-D.; He, X.-F.; Xia, W.; Zhang, Y.-Q.; Liang, H.; Reddy, C. V. S.; Cao, R.-H.; Qiu, L.-Q. Pd-Catalyzed Asymmetric Suzuki−Miyaura Coupling Reactions for the Synthesis of Chiral Biaryl Compounds with a Large Steric Substituent at the 2-Position. *Beilstein J. Org. Chem.* **16**, 966−973(2020).

6. Ji, W.-Q.; Wu,H.-H.; Zhang,J.-L. Axially Chiral Biaryl Monophosphine Oxides Enabled by Palladium/WJ-Phos-Catalyzed Asymmetric Suzu ki−Miyaura Cross-Coupling. *ACS Catal.* **10**, 1548−1554 (2020) .
7. (a) Tang, W.-J.; Patel, N. D.; Xu, G.-Q.; Xu, X.-B.; Savoie, J.; Ma, S.-L.; Hao, M.-H.; Keshipeddy, S.; Capacci, A. G.; Wei, X.-D.; Zhang, Y.-D.; Gao, J. J.; Li, W.-J.; Rodriguez, S.; Lu, B. Z.; Yee, N. K.; Senanayake, C. H. Efficient Chiral Monophosphorus Ligands for Asymmetric Suzuki−Miyaura Coupling Reactions. *Org. Lett.* **14**, 2258−2261(2012). (b) Xu, G.-Q.; Fu, W.-Z.; Liu, G.-D.; Senanayake, C. H.; Tang, W.-J. Efficient Syntheses of Korupensamines A, B and Michellamine B by Asymmetric Suzuki−Miyaura Coupling Reactions. *J. Am. Chem. Soc.* **136**, 570−573(2014). (c) Yang, X.-T.; Xu, G.-Q.; Tang, W.-J.;Efficient Synthesis of Chiral Biaryls via Asymmetric Suzuki−Miyaura Cross-Coupling of Ortho-Bromo Aryl Triflates. *Tetrahedron* **72**, 5178−5183(2016). (d) Yang, H.; Sun, J.-W.; Gu, W.; Tang, W.-J. Enantioselective Cross Coupling for Axially Chiral Tetra-Ortho-Substituted Biaryls and Asymmetric Synthesis of Gossypol. *J. Am. Chem. Soc.* **142**, 8036−8043(2020).
8. Byrne, L.; Sköld, C.; Norrby, P.-O.; Munday, R. H.; Turner, A. R.; Smith, P. D. Enantioselective Synthesis of Atropisomeric Biaryls Using Biaryl 2,5-Diphenylphospholanes as Ligands for Palladium-Catalysed Suzuki−Miyaura Reactions. *Adv. Synth. Catal.* **363**, 259−267(2021)
9. (a) Bermejo, A.; Ros, A.; Fernández, R.; Lassaletta, J. M. C2-Symmetric Bis-Hydrazones as Ligands in the Asymmetric Suzuki− Miyaura Cross-Coupling. *J. Am. Chem. Soc.* **130**, 15798−15799(2008). (b) Ros, A.; Estepa, B.; Bermejo, A.; Alvarez, E.; Fernández, R.; Lassaletta, J. M. Phosphino Hydrazones as Suitable Ligands in the Asymmetric Suzuki−Miyaura Cross-Coupling. *J. Org. Chem.* **77**, 4740−4750(2012).
10. Zhang, S.-S.; Wang, Z.-Q.; Xu, M.-H.; Lin, G.-Q. Chiral Diene as the Ligand for the Synthesis of Axially Chiral Compounds via Palladium-Catalyzed Suzuki−Miyaura Coupling Reaction. *Org. Lett.* **12**, 5546−5549(2020).
11. Wu, L.-L.; Salvador, A.; Ou, A.; Shi, M.-W.; Skelton, B. W.; Dorta, R. Monodentate Chiral N-Heterocyclic Carbene−Palladium-Catalyzed Asymmetric Suzuki−Miyaura and Kumada Coupling. *Synlett* **24**, 1215−1220(2013).
12. Shen, D.; Xu, Y.-J.; Shi, S.-L. A Bulky Chiral N-Heterocyclic Carbene Palladium Catalyst Enables Highly Enantioselective Suzuki−Miyaura Cross-Coupling Reactions for the Synthesis of Biaryl Atropisomers. *J. Am. Chem. Soc.* **141**, 14938−14945(2019).
13. Chatterjee, A.; Mallin, H.; Klehr, J.; Vallapurackal, J.; Finke, A. D.; Vera, L.; Marsh, M.; Ward, T. R. An Enantioselective Artificial Suzukiase Based on the Biotin−Streptavidin Technology. *Chem. Sci.* **7**, 673−677(2016).
14. (a) Uozumi, Y.; Matsuura, Y.; Arakawa, T.; Yamada, Y. M. A. Asymmetric Suzuki−Miyaura Coupling in Water with a Chiral Palladium Catalyst Supported on an Amphiphilic Resin. *Angew. Chem., Int. Ed*. **48**, 2708−2710(2009). (b) Uozumi, Y.; Matsuura, Y.; Suzuka, T.; Arakawa, T.; Yamada, Y. M. A. Palladium-Catalyzed Asymmetric Suzuki−Miyaura Cross

Coupling with Homochiral Phosphine Ligands Having Tetrahydro 1H-Imidazo[1,5-a]Indole Backbone. *Synthesis*, **49**, 59–68(2016).(c) Sawai, K.; Tatumi, R.; Nakahodo, T.; Fujihara, H. Asymmetric Suzuki–Miyaura Coupling Reactions Catalyzed by Chiral Palladium Nanoparticles at Room Temperature. *Angew. Chem., Int. Ed.* **47**, 6917–6919(2008). (d) Mori, K.; Kondo, Y.; Yamashita, H. Synthesis and Characterization of FePd Magnetic Nanoparticles Modified with Chiral BINAP Ligand as a Recoverable Catalyst Vehicle for the Asymmetric Coupling Reaction. *Phys. Chem. Chem. Phys.* **11**, 8949–8954(2009). (e) Yamamoto, T.; Akai, Y.; Nagata, Y.; Suginome, M. Highly Enantioselective Synthesis of Axially Chiral Biarylphosphonates: Asymmetric Suzuki–Miyaura Coupling Using High-Molecular Weight, Helically Chiral Polyquinoxaline-Based Phosphines. *Angew. Chem., Int. Ed.* **50**, 8844–8847(2011). (f) Suginome, M.; Yamamoto, T.; Nagata, Y.; Yamada, T.; Akai, Y. Catalytic Asymmetric Synthesis Using Chirality-switchable Helical Polymer as a Chiral Ligand. *Pure Appl. Chem.* **84**, 1759–1769(2012). (g) Akai, Y.; Konnert, L.; Yamamoto, T.; Suginome, M. Asymmetric Suzuki–Miyaura Cross-Coupling of 1-Bromo-2-Naphthoates Using the Helically Chiral Polymer Ligand PQXphos. *Chem. Commun.* **51**, 7211–7214(2015). (h) Nagata, Y.; Kuroda, T.; Takagi, K.; Suginome, M. Ether Solvent Induced Chirality Inversion of Helical Poly(Quinoxaline-2,3-Diyl)s Containing L-Lactic Acid Derived Side Chains. Chem. Sci. **5**, 4953–4956(2014). (i) Nagata, Y.; Takeda, R.; Suginome, M. Asymmetric Catalysis in Chiral Solvents: Chirality Transfer with Amplificationof Homochirality through a Helical Macromolecular Scaffold. *ACS Cent. Sci.* **5**, 1235–1240(2019). (j) Ikeda, S.; Takeda, R.; Fujie, T.; Ariki, N.; Nagata, Y.; Suginome, M. Protected Amino Acids as a Nonbonding Source of Chirality in Induction of Single-Handed Screw-Sense to Helical Macromolecular Catalysts. *Chem. Sci.* **12**, 8811–8816(2021).

15. (a) Han, F.-S. Transition-Metal-Catalyzed Suzuki–Miyaura Cross Coupling Reactions: A Remarkable Advance from Palladium to Nickel Catalysts. *Chem. Soc. Rev.* **42**, 5270–5298(2013). (b) Cooper, A. K.; Burton, P. M.; Nelson, D. J. Nickel versus Palladium in Cross-Coupling Catalysis: On the Role of Substrate Coordination to Zerovalent Metal Complexes. *Synthesis* **52**, 565–573(2020).
16. (a) Tasker, S. Z., Standley, E. A.; Jamison, T. F. Recent advances in homogeneous nickel catalysis. *Nature* **509**, 299–309 (2014). (b) Ananikov, V. P. Nickel: the “spirited horse” of transition metal catalysis. *ACS Catal.* **5**, 1964–1971 (2015).
17. For selected review: (a) He, Y.; Yang, X.-T.; Tang, W.-J. Transition-metal catalyzed asymmetric carbon-carbon cross-coupling with chiral ligands. *Tetrahedron* **72**, 6143-6174(2016). (b) Hazari, N.; Melvin, P. R.; Beromi, M. M. Well-Defined Nickel and Palladium Precatalysts for Cross-Coupling. *Nat. Rev. Chem*. **1**, 25(2017).
18. For representative works on Ni-SMC: (a) Percec, V.; Bae, J.-Y.; Hill, D. H. Aryl Mesylates in Metal Catalyzed Homocoupling and Cross-Coupling Reactions. 2. Suzuki Type Nickel-Catalyzed Cross-Coupling of Aryl Arenesulfonates and Aryl Mesylates with Arylboronic Acids. *J. Org. Chem.* **60**, 1060–1065(1995). (b) Saito, S.; Oh-tani, S.; Miyaura, N. Synthesis of Biaryls via a Nickel(0)-Catalyzed Cross-Coupling Reaction of Chloroarenes with Arylboronic Acids. *J. Org. Chem.* **62**, 8024–8030(1997). (c) Inada, K.; Miyaura, N. Synthesis of Biaryls via Cross-Coupling Reaction of Arylboronic Acids with Aryl Chlorides Catalyzed by NiCl 2 /Triphenylphosphine Complexes. *Tetrahedron* **56**, 8657–8660(2000).

(d) Quasdorf, K. W.; Tian, X.; Garg N. K.; Cross-Coupling Reactions of Aryl Pivalates with Boronic Acids. *J. Am. Chem. Soc.* **130**, 14422–14423(2008) (e)Quasdorf, K. W.; Riener, M.; Petrova, K. V.; Garg, N. K. Suzuki-Miyaura Coupling of Aryl Carbamates, Carbonates, and Sulfamates. *J. Am. Chem. Soc.* **131**, 49, 17748–17749(2009) (f) Molander, G. A.; Beaumard, F. Nickel-Catalyzed C-O Activation of Phenol Derivatives with Potassium Heteroaryltrifluoroborates *Org. Lett.* **12**, 4022-4025(2010). (g) Quasdorf, K. W.; Antoft-Finch, A.; Liu, P.; Silberstein, A. L.; Komaromi, A.; Blackburn, T.; Ramgren, S. D.; Houk, K. N.; Snieckus, V.; Garg, N. K. Suzuki Miyaura Cross-Coupling of Aryl Carbamates and Sulfamates: Experimental and Computational Studies. *J. Am. Chem. Soc.* **133**, 6352–6363(2011) (h) Zhang, N.; Hoffman, D. J.; Gutsche, N.; Gupta, J.; Percec, V. Comparison of Arylboron-Based Nucleophiles in Ni-Catalyzed Suzuki–Miyaura Cross-Coupling with Aryl Mesylates and Sulfamates. *J. Org. Chem.* **77**, 5956–5964(2012). (i) Leowanawat, P.; Zhang, N.; Safi, M.; Hoffman, D., J.; Fryberger, M. C.; George, A.; Percec, V.; trans-Chloro(1-Naphthyl)bis(triphenylphosphine)nickel(II)/PCy_3 Catalyzed Cross-Coupling of Aryl and Heteroaryl Neopentylglycolboronates with Aryl and Heteroaryl Mesylates and Sulfamates at Room Temperature. *J. Org. Chem.* **77**, 2885–2892(2012). (j) Ramgren, S. D.; Hie, L.; Ye, Y.-X.; Garg, N. K. Nickel-Catalyzed Suzuki–Miyaura Couplings in Green Solvents. *Org. Lett.* **15**, 3950–3953(2013). (k) Li, X.-J.; Zhang, J.-L.; Geng, Y.; Zhong, J. Nickel-Catalyzed Suzuki–Miyaura Coupling of Heteroaryl Ethers with Arylboronic Acids *J. Org. Chem.* 78, 5078–5084(2013). (l) Jezorek, R. L.; Zhang, N.; Leowanawat, P.; Bunner, M. H.; Gutsche, N.; Pesti, A. K. R.; Olsen, J. T.; Percec, V. Air-Stable Nickel Precatalysts for Fast and Quantitative Cross Coupling of Aryl Sulfamates with Aryl Neopentylglycolboronates at Room Temperature *Org. Lett.* **16**, 6326–6329(2014) (m) Mastalir, M.; Stoger, B.; Pittenauer, E.; Allmaier, G.; Kirchner, K.; Air-Stable Triazine-Based Ni(II) PNP Pincer Complexes As Catalysts for the Suzuki–Miyaura Cross-Coupling. *Org. Lett.* **18**, 3186–3189(2016)

19. Zhang, S.-Q.; Hong, X.; Mechanism and Selectivity Control in Ni- and Pd-Catalyzed Cross-Couplings Involving Carbon–Oxygen Bond Activation. *Acc.Chem.Res.* **54**, 2158–2171(2021).
20. Yang, J.; Neary, M. C.; Diao, T.-N.; ProPhos: A Ligand for Promoting Nickel-Catalyzed Suzuki-Miyaura Coupling Inspired by Mechanistic Insights into Transmetalation. https://doi.org/10.1021/jacs.4c00370
21. Chirik, P. J.; Engle,K. M.; Simmons, E. M.; Wisniewski, S. R. Collaboration as a Key to Advance Capabilities for Earth-Abundant Metal Catalysis. *Org. Process Res. Dev.* **27**, 1160–1184(2023).
22. (a) Taylor, C. J. *et al.* A Brief Introduction to Chemical Reaction Optimization. *Chem. Rev.* **123**, 3089–3126 (2023). (b) Shields, B. J. *et al.* Bayesian reaction optimization as a tool for chemical synthesis. *Nature* **590**, 89–96 (2021). (c) Zhang, Z.-J. *et al.* Data-driven design of new chiral carboxylic acid for construction of indoles with C-central and C–N axial chirality via cobalt catalysis. *Nat. Commun.* **14**, 3149 (2023). (d) Rinehart, N. I. *et al.* A machine-learning tool to predict substrate-adaptive conditions for Pd-catalyzed C–N couplings. *Science* **381**, 965–972 (2023).
23. (a) Pesciullesi, G., Schwaller, P., Laino, T. & Reymond, J.-L. Transfer learning enables the molecular transformer to predict regio- and stereoselective reactions on carbohydrates.

Nat. Commun. **11**, 4874 (2020). (b) Wen, M., Blau, S. M., Xie, X., Dwaraknath, S. & Persson, K. A. Improving machine learning performance on small chemical reaction data with unsupervised contrastive pretraining. *Chem. Sci.* **13**, 1446–1458 (2022).

24. Li, W. & Zhang, J. Sadphos as Adaptive Ligands in Asymmetric Palladium Catalysis. *Acc. Chem. Res.* **57**, 489–513 (2024).
25. Xu, L.-C. *et al.* Towards Data-Driven Design of Asymmetric Hydrogenation of Olefins: Database and Hierarchical Learning. *Angew. Chem. Int. Ed.* **60**, 22804–22811 (2021).
26. Ertl, P. & Schuffenhauer, A. Estimation of synthetic accessibility score of drug-like molecules based on molecular complexity and fragment contributions. *J. Cheminform.* **1**, 8 (2009).